Decoding Auxetics: Machine Learning for Interrelating Poisson's Ratio and Unit Cell Geometry

Kamakshi Subramanian, Evan Hutchinson, Karen Andre

5/13/25

1.052 Advancing Mechanics and Materials via Machine Learning

Professor Markus J. Buehler

Abstract

Metamaterials offer unique mechanical properties that make them of merit to study. They may have specific responses to loading, desirable impact absorption, or high strength to weight ratios that make them shine in applications of interest. This paper looks at auxetic metamaterials specifically, which have negative Poisson's ratios and are constructed of repeated unit cell geometries. The broad design space for auxetic unit cells has led researchers to employ machine learning as a means of relating Poisson's ratio to unit cell geometry. This investigation employs a series of different approaches for relating geometry to Poisson's ratio, and finds a novel set of equations that serve as explainable models for the influence of unit cell design on whether a material will perform like an auxetic or not, opening doors to a more accessible design workflow for auxetic materials.

Keywords: Auxetic, Metamaterial, Symbolic Regression, Variational Autoencoder, Machine Learning

1. Introduction

Computational tools have various use cases throughout the engineering design process. Finite element analysis helps with understanding structural responses to loading, computational fluid dynamics helps understand fluid flows, and topology optimization can help optimize structural performance while minimizing material use or cost. However, the cost of software licenses or the compute power necessary make these sophisticated computational tools inaccessible for some users. In the absence of access to these tools, first principles judgements and approximations may offer insight, but after a certain level of complexity the tools once again become necessary.

Machine learning has been leveraged to develop surrogate models to provide greater insights than simulations can provide [8], as well as to provide less intensive alternatives to finite element simulations [4]. This paper aims to provide another application of machine learning to engineering design, with the chief goal of producing readily explainable models that have lower computational cost than running a dedicated simulation software.

The focus of this study is on the design of auxetic metamaterials. Auxetic metamaterials differ from traditional materials because they have a negative Poisson's ratio, which is the ratio of transverse strain to axial strain. When loaded, materials with positive Poisson's ratio will narrow in the transverse direction as they lengthen in the axial direction, like a rubber band. Auxetics expand in the transverse direction instead. This property gives auxetic metamaterials advantageous properties of low density, high energy absorption, and high shear resistance [6].

To develop a model that can relate unit cell geometry to Poisson's ratio in an explainable fashion, a symbolic regression model was trained, and results were then compared to those of a traditional feedforward neural network. Following evaluation of the regression model solving the forward problem, a solution to the inverse problem of mapping Poisson's ratio to geometry was attempted using a variational autoencoder on unit cell images supplemented with text data.

2. Background

2.1 Understanding Auxetics

The property that determines whether a material is an auxetic or not is the Poisson's ratio, ν, which relates the transverse strain $d\varepsilon_{trans}$ to the axial strain $d\varepsilon_{axial}$ under loading (Equation 1). A piece of elastic material that becomes narrower while being pulled apart is an example of the Poisson's ratio equation in action. Under some positive elongation ($d\varepsilon_{axial} > 0$), the transverse dimension of the segment contracts and becomes narrower ($d\varepsilon_{trans} < 0$), leading to the positive Poisson's ratio that characterizes it and the majority of other naturally occurring materials.

$$\nu = -\frac{d\varepsilon_{trans}}{d\varepsilon_{axial}} \quad (1)$$

A familiar naturally occurring example of a material with a Poisson's ratio of 0 is cork, which is why it is used to seal wine bottles. The material experiences essentially no lateral deformation upon axial loading, which is why it can be pressed into a wine bottle and hold its shape, rather than expanding or narrowing out under pressure.

Auxetic materials achieve a negative Poisson's ratio by repeating a carefully selected unit cell geometry throughout some bulk structure. These unit cells can take on a range of geometries, ranging from a tessellated hexagon pattern to a series of irregular ovals or triangles. To explore the design space, this investigation will focus specifically on re-entrant unit cell geometries, as their full structure can be characterized by only 4 parameters: slant cell length, vertical cell height, cell angle, and cell thickness.

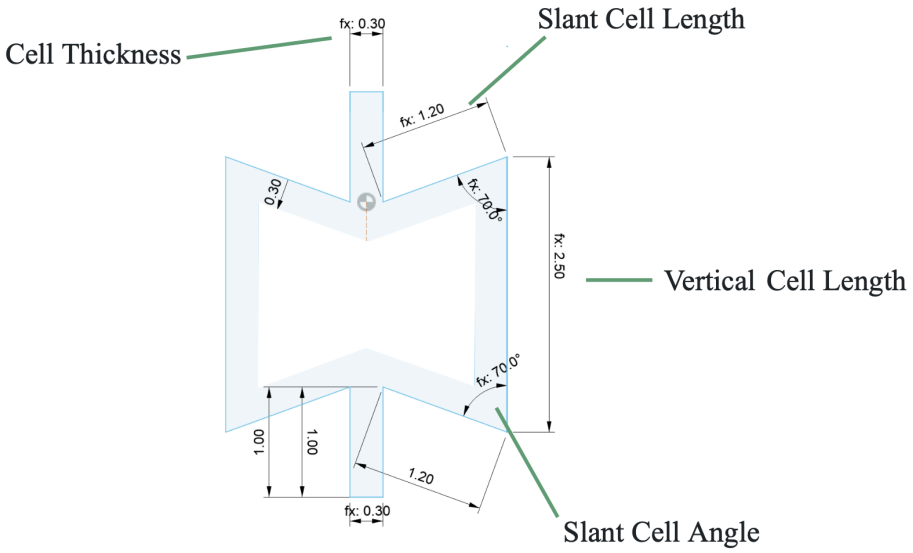

Figure 1: Schematic representation of re-entrant auxetic unit cell geometry.

Being able to relate the geometry of auxetics to their Poisson's ratio without finite element simulations will accelerate the design process, and may allow for rapid generation of valid auxetic materials that fulfill constraints specified by the user.

2.2 Related Work

Related investigations navigate the auxetic design space by relying solely on domain knowledge to inform unit cell design [5], or implemented topology optimization [11]. Of the studies that use machine learning to predict properties and generate designs, some utilize convolutional neural networks to predict deformation from FEA results over different geometries [10], use genetic algorithms to generate valid geometries by permuting encodings of the material structure [2,9], or use Gaussian Process Regression alongside SHAP analysis to generate structures with explainable models [1,7].

The findings of each of these studies either serve to characterize the relative importance of different parameters in the performance of an auxetic material, or generate new geometries based on domain knowledge. However, there is still a gap in the literature that provides a simple mathematical equation that can be used in hand-calculations to map the relation between unit cell geometry and Poisson's ratio. These studies instead use Shapley Additive explanation (SHAP) to find trends in the data or relative importance, still lean on finite element simulations at some stage of result generation, or rely on common effective but non-interpretable black box models. The studies do not consider a means of producing equations that match a specific unit cell geometry to its Poisson's ratio. As such, the following investigation into the relationship between re-entrant auxetic unit cell geometry and Poisson's ratio produces a set of candidate equations for relating geometry to property, compares these results to standard methodologies, and attempts to solve the inverse problem to generate properties from a desired Poisson's ratio and a set of constraints.

3. Methods

3.1 Regression Model Overview

The dataset used in this investigation was generated by researchers at the University of Rhode Island [7], where it relates a re-entrant auxetic unit cell's slant length, cell angle, vertical cell height, and cell thickness to the Poisson's ratio for 8096 samples. As a benchmark for result quality, a traditional feedforward neural network (MLP) was trained on this dataset using a 70% train, 15% validation, and 15% test split. The model architecture is outlined below.

```
Neural Network Architecture Summary:
----------------------------------------------------------------------
      Layer (type)        Output Shape         Param #     Tr. Param #
======================================================================
          Linear-1         [5666, 64]             320             320
            ReLU-2         [5666, 64]               0               0
          Linear-3         [5666, 32]           2,080           2,080
            ReLU-4         [5666, 32]               0               0
          Linear-5         [5666, 16]             528             528
            ReLU-6         [5666, 16]               0               0
          Linear-7          [5666, 1]              17              17
======================================================================
Total params: 2,945
Trainable params: 2,945
Non-trainable params: 0
----------------------------------------------------------------------
```

Figure 2: Summary of feedforward neural network architecture used for inference of Poisson's ratio.

The regression model contains three hidden layers with ReLU activation functions. The model was trained for 96 epochs with a learning rate of 0.001. To prevent data leakage, the train, test, and validation splits were scaled separately, and data loaders were added to allow for batching and shuffling. An MSE loss function alongside the Adam optimizer was used.

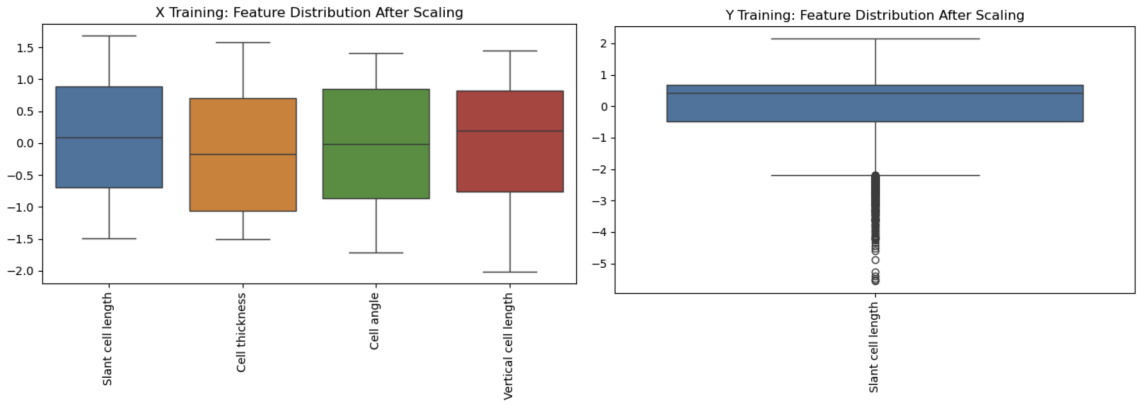

Figure 3: Feature distributions after scaling for training data. StandardScalers were fitted on the training, validation, and testing data to remove the mean and scale to unit variance.

3.2 Symbolic Regression Overview

Following training and validation of the traditional black-box regression model, the symbolic regression model was trained next. The PySR library was used because it is an open-source, high performance symbolic regression package that is optimized for low dimensional datasets [3]. The working principle of the library being a genetic algorithm that randomly generates candidate equations, evaluates them, permutes them, then re-generates them either from scratch or through some form of combination with other candidate equations.

The hyperparameters for genetic algorithms differ from those of traditional neural network architectures. Rather than adjusting things like activation function or model depth, a genetic algorithm can be modified by changing how many equations are generated and mutated within a single population, how many separate populations of equations are being trained at once, as well as how complex the equations should be or which mathematical operators can be included within the equations produced.

Data was handled identically to the base regression model in section 3.1, and the PySR model was trained using a population size of 100 across 30 different populations, and 200 iterations of the algorithm to run. Deterministic was set to True to ensure reproducibility of results and the model was provided with the four basic binary operators as well as the square root unary operator. Parsimony was set to 1e-4 and maxsize was set to 40 to allow equations of greater complexity, and equations were selected for accuracy only. Future efforts will also factor complexity into model choice.

3.3 Inverse Problem using VAE

After generating mathematical expressions relating geometry to Poisson's ratio, the inverse problem of relating Poisson's ratio to re-entrant unit cell geometry was attempted. A variational autoencoder was used to first give the model an idea of what re-entrant unit cell geometries look like alongside their Poisson's ratios, and its outputs would be supplemented with text data that provide more constraints on what constitutes a valid result. As the dataset is a set of tabulated numerical data, the first step of training the VAE was changing the representation of the data from text to images. A program was written that automatically drew each sample from the dataset based on its geometric parameters. Training and test data were tuples of a given unit cell's image and its corresponding Poisson's ratio.

From these images, the model would learn latent representations of geometric parameters. Image data passed through 3 convolutional layers in the encoder and decoder, while the numerical constraint data would be passed through 2 fully connected layers in the encoder and decoder respectively.

4. Results and Discussion

4.1 Baseline Results using Feedforward Neural Network

To have a reference point which the mathematical equations output by section 3.2's symbolic regression model could be compared with, the regression model from section 3.1 was trained for 96 epochs.

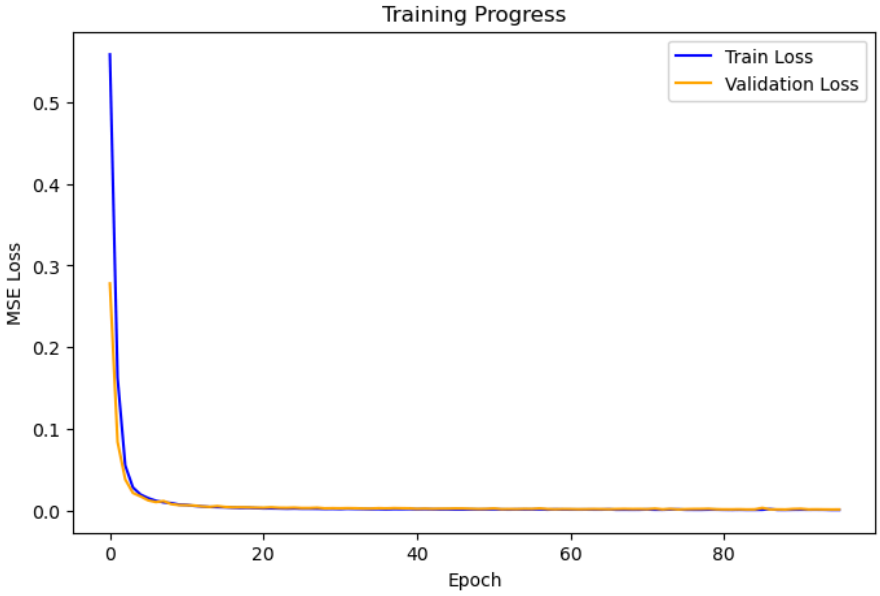

Figure 4: MSE loss curves for the feedforward neural network in section 3.1. Training and validation losses were low, indicating high model performance.

After training, the model was evaluated on the test dataset to have an R^2 score of 0.999, MAE of 0.003, and RMSE of 0.004.

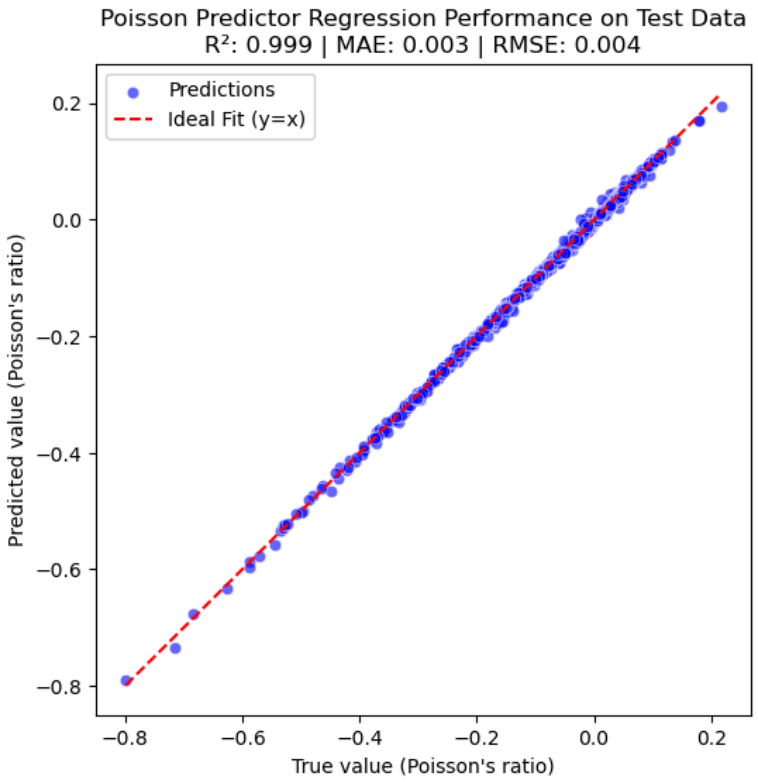

Figure 5: Predicted value vs true value for the MLP regression model on the testing data.

The model succeeded in capturing the relationship between unit cell geometry and Poisson's ratio very well. Given that Poisson's ratio is defined by relating transverse strain to axial strain, and both strains are related to the geometric changes experienced by the sample under loading, it was expected that the model would succeed in understanding how the unloaded geometry of an auxetic or traditional unit cell would be changed under applied force. This high performance on the dataset is the gold standard for what the symbolic regression and inverse model should be compared with.

4.2 Interpretable Results from Symbolic Regression

Outputs from training the symbolic regression model take the form of a set of equations alongside a score that indicates how well they performed during evaluation. This score is defined as the negative derivative of log loss with respect to complexity for a given equation, where the complexity is determined by how many terms are in the equation and which mathematical operators are used. Per training run, 14 to 16 equations are output in order of increasing complexity, and the PySR library automatically drops or includes terms in a given expression based on how important they are. Herein, something similar to SHAP analysis took place, as the general trends of which parameters appeared in the equations can be considered to understand the broader importance of that property to an auxetic material's performance. For example, slant cell length and cell angle appear in every output equation regardless of complexity, whereas cell thickness only tends to appear in more complex equations. It is concluded then that slant angle is more important to a unit cell's auxetic properties, whereas something like cell length is a higher order term that increases the model's accuracy but is not a critical example. This is in agreement

with Oladipo et. al's investigation using traditional regression and SHAP analysis [7], where slant cell length and cell angle were determined to be the most important inputs, while cell thickness was judged to be the least critical.

Different training parameters were experimented with to boost performance. Training the model for a higher number of iterations, increasing the number of disparate populations, and changing the scoring criteria which selected equations were all adjusted in order to make the model accurate while also making it robust. A simple equation such as $Slant\ Cell\ Length\ *\ -0.6635$ had poorer performance, while the best performing equation (Equation 2) was also the most complex.

$$\frac{(-0.082)(Cell\ Thickness+0.182+\frac{Slant\ Cell\ Length+1.203}{-0.724(Cell\ Angle)(Cell\ Angle-0.126(Slant\ Cell\ Length))}+0.677)(2.23(Cell\ Angle)-0.724(Slant\ Cell\ Length)-2.233)+0.567)}{Vertical\ Cell\ Length+3.184}-0.515 \quad (2)$$

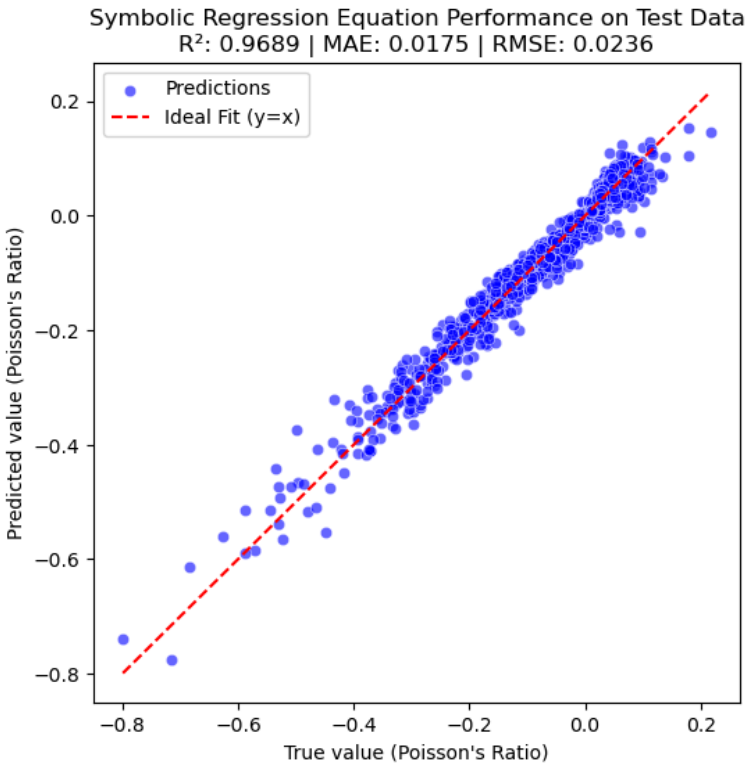

Figure 6: Predicted value vs true value for Equation 2 (best performing equation from symbolic regression analysis) on the testing data.

This equation had an R^2 score of 0.969 and RMSE of 0.0236, indicating comparable high performance to the regression model but with the added benefit of being an interpretable mathematical expression that generalizes to any re-entrant unit cell. To further validate the model's results, a finite element simulation was attempted, though TPU was not part of the available software's material library, leading to discrepancies between what the simulation predicted versus the ground truth, as this was the material each unit cell in the study's dataset was composed of.

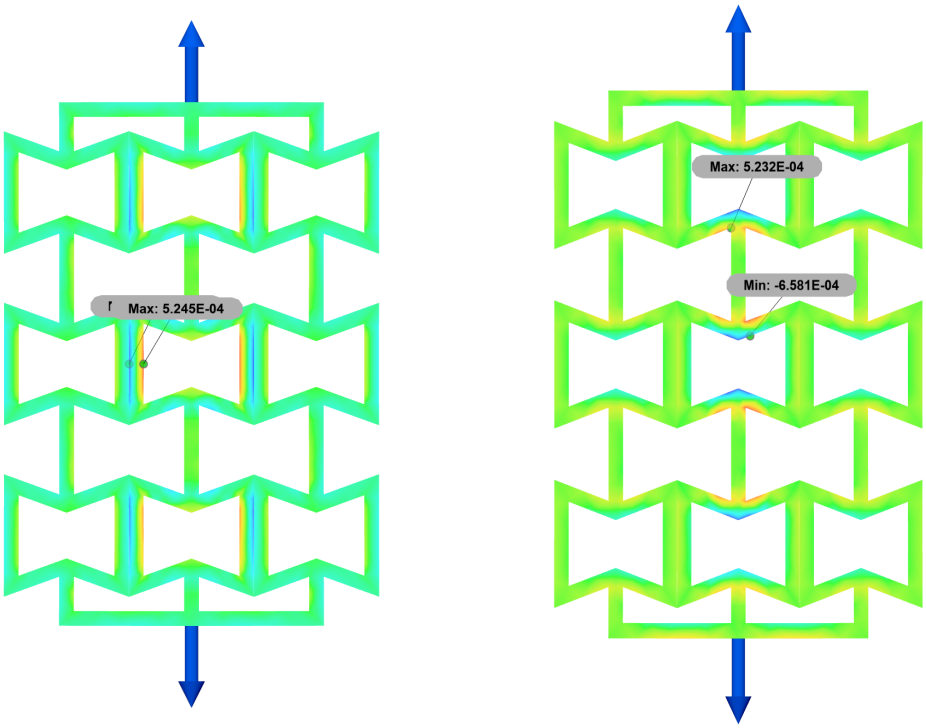

Figure 7: Finite element simulation results for sample 39 of the dataset showing maximum axial strain (left) and transverse strain (right). However, TPU was missing from the simulation software's material library, leading to the simulated Poisson's ratio being an order of magnitude higher than the ground truth value.

4.3 Inverse Problem using Image Data

After a solution to the forward problem was generated, the inverse problem was next attempted using the methods outlined in section 3.3. However, the model's predictions were poor due to its inability to distinguish between unit cells with different geometries. Scaling the images to the same size was attempted, however these important geometric features (such as vertical cell length) remained difficult to determine from the image representations of the geometric data. Additionally, the cell thickness only varied by one unit throughout the dataset, and a subtle difference like this was not captured by the model, likely due to the small image size and similar line thickness differences.

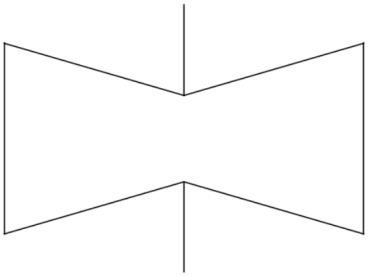

Slant cell length	20.000000
Cell thickness	2.200000
Cell angle	70.000000
Vertical cell length	25.000000
Poisson's ratio	−0.714003

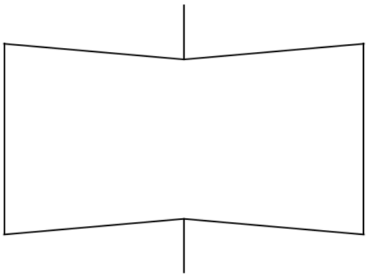

Slant cell length	6.00000
Cell thickness	2.80000
Cell angle	70.00000
Vertical cell length	25.00000
Poisson's ratio	0.08319

Figure 8: Input images (left) versus true material properties (right). The VAE failed to capture the subtle differences between different unit cell geometries, leading it to be a suboptimal way of solving the inverse problem of generating the remaining geometric properties from some Poisson's ratio and constrained image data.

Across the model architectures tested for the forward and inverse problems, it is seen that the forward problem is tractable both in the classical paradigm of black box regression models, and in the domain of explainable AI via symbolic regression. The methods for the inverse problem did not yield similarly successful results, however, due to the chosen data representation and model architecture struggling to capture the subtle differences between samples needed to precisely predict their Poisson's ratios.

The traditional regression model was able to determine the relationship between the unit cell geometry and the Poisson's ratio with little to no error, at the expense of little to no interpretability without additional steps like SHAP analysis. The symbolic regression model produced over 60 candidate equations to relate Poisson's ratio for auxetics to unit cell geometry, with the best performing equation having 3% lower performance on the test data than the regression model but offering much greater interpretability. Difficulties with model architecture and data representation hindered the accomplishment of an inverse solution.

4.4 Limitations and Future Work

The traditional regression model did not encounter significant obstacles to achieving high performance on the dataset. Similarly, once hyperparameters were optimized for the symbolic regression model, performance was high as well.

Due to the sheer number of permutations that go into training the symbolic regression model, this study was limited to lower population numbers and iteration counts, alongside more simple mathematical expressions that could be involved in solutions. Future studies with access to greater computational resources could experiment with more mathematically complex expressions that use fewer or nonlinear terms (such as trigonometric operators), as well as with punishing equation complexity as a means of finding the simplest relationship possible and analyzing all solutions on the Pareto front. Additionally, future studies should expand to different unit cell geometries outside of re-entrant ones, even possibly striving for a solution that generalizes to all geometries. Adding material to the dataset prior to training, or performing transfer learning to allow for material-specific equation generation is another avenue that this work could travel down in future investigations.

For the inverse problem, future studies should look at further image transformations or alternative representations altogether (such as numerical data or multimodal inputs) in order to allow for constrained generation of auxetics given a target Poisson's ratio. They should also consider other generative model architectures, such as conditional GANs.

5. Conclusions

The relationship between unit cell geometry and Poisson's ratio has been investigated before. However, this study aims to improve upon explainability by using symbolic regression to derive mathematical expressions that provide comparable predictions to the high-performing black box models used in related work. These expressions had comparable performance with predicting Poisson's ratios for various re-entrant unit cells, done without the need to include PDEs in the loss function or employ a simulation software that may have high monetary or computational barriers to usage.

This study’s work can be transferred over to other auxetic material unit cell geometries, assuming the dataset maps characteristic features to Poisson's ratio. While currently limited to a single material, future work could expand it to any arbitrary Young’s modulus. The inverse problem remains unsolved using the method of the variational autoencoder outlined in this paper, and additional investigation should take place in order to build upon the work here to solve it.

Acknowledgments

The authors would like to acknowledge Professor Markus Buehler, Dr. Alireza Ghafarollahi, and Michael Hsu for their guidance on this project and help with brainstorming expansions to the current body of work.

References

[1] Afdhal, Jirousek, O., Palar, P. S., Falta, J., and Dwianto, Y. B., 2023, "Design Exploration of Additively Manufactured Chiral Auxetic Structure Using Explainable Machine Learning," Materials & Design, 232, p. 112128. https://doi.org/10.1016/j.matdes.2023.112128.

[2] Chang, Y., Wang, H., and Dong, Q., 2022, "Machine Learning-Based Inverse Design of Auxetic Metamaterial with Zero Poisson's Ratio," Materials Today Communications, 30, p. 103186. https://doi.org/10.1016/j.mtcomm.2022.103186.

[3] Cranmer, M., 2023, "Interpretable Machine Learning for Science with PySR and SymbolicRegression.Jl." https://doi.org/10.48550/arXiv.2305.01582.

[4] Cuomo, S., Di Cola, V. S., Giampaolo, F., Rozza, G., Raissi, M., and Piccialli, F., 2022, "Scientific Machine Learning Through Physics–Informed Neural Networks: Where We Are and What's Next," J Sci Comput, 92(3), p. 88. https://doi.org/10.1007/s10915-022-01939-z.

[5] Masters, I. G., and Evans, K. E., 1996, "Models for the Elastic Deformation of Honeycombs," Composite Structures, 35(4), pp. 403–422. https://doi.org/10.1016/S0263-8223(96)00054-2.

[6] Momoh, E. O., Jayasinghe, A., Hajsadeghi, M., Vinai, R., Evans, K. E., Kripakaran, P., and Orr, J., 2024, "A State-of-the-Art Review on the Application of Auxetic Materials in Cementitious Composites," Thin-Walled Structures, 196, p. 111447. https://doi.org/10.1016/j.tws.2023.111447.

[7] Oladipo, B., Matos, H., Krishnan, N. M. A., and Das, S., 2023, "Integrating Experiments, Finite Element Analysis, and Interpretable Machine Learning to Evaluate the Auxetic Response of 3D Printed Re-Entrant Metamaterials," Journal of Materials Research and Technology, 25, pp. 1612–1625. https://doi.org/10.1016/j.jmrt.2023.06.038.

[8] Smith, T. N., "Data Driven Surrogate Models for Faster SPICE Simulation of Power Supply Circuits."

[9] Wang, M., Sun, S., and Zhang, T.-Y., 2023, "Machine Learning Accelerated Design of Auxetic Structures," Materials & Design, 234, p. 112334. https://doi.org/10.1016/j.matdes.2023.112334.

[10] Wilt, J. K., Yang, C., and Gu, G. X., 2020, "Accelerating Auxetic Metamaterial Design with Deep Learning," Advanced Engineering Materials, 22(5), p. 1901266. https://doi.org/10.1002/adem.201901266.

[11] Wu, J., Luo, Z., Li, H., and Zhang, N., 2017, “Level-Set Topology Optimization for Mechanical Metamaterials under Hybrid Uncertainties,” Computer Methods in Applied Mechanics and Engineering, 319, pp. 414–441. https://doi.org/10.1016/j.cma.2017.03.002.